

## Measurements of Z-Boson Resonance Parameters in $e^+e^-$ Annihilation

G. S. Abrams,<sup>(1)</sup> C. E. Adolphsen,<sup>(2)</sup> D. Averill,<sup>(4)</sup> J. Ballam,<sup>(3)</sup> B. C. Barish,<sup>(5)</sup> T. Barklow,<sup>(3)</sup> B. A. Barnett,<sup>(6)</sup> J. Bartelt,<sup>(3)</sup> S. Bethke,<sup>(1)</sup> D. Blockus,<sup>(4)</sup> G. Bonvicini,<sup>(7)</sup> A. Boyarski,<sup>(3)</sup> B. Brabson,<sup>(4)</sup> A. Breakstone,<sup>(8)</sup> J. M. Brom,<sup>(4)</sup> F. Bulos,<sup>(3)</sup> P. R. Burchat,<sup>(2)</sup> D. L. Burke,<sup>(3)</sup> R. J. Cence,<sup>(8)</sup> J. Chapman,<sup>(7)</sup> M. Chmeissani,<sup>(7)</sup> D. Cords,<sup>(3)</sup> D. P. Coupal,<sup>(3)</sup> P. Dauncey,<sup>(6)</sup> H. C. DeStaeblcr,<sup>(3)</sup> D. E. Dorfan,<sup>(2)</sup> J. M. Dorfan,<sup>(3)</sup> D. C. Drewcr,<sup>(6)</sup> R. Elia,<sup>(3)</sup> G. J. Feldman,<sup>(3)</sup> D. Fernandes,<sup>(3)</sup> R. C. Field,<sup>(3)</sup> W. T. Ford,<sup>(9)</sup> C. Fordham,<sup>(3)</sup> R. Frey,<sup>(7)</sup> D. Fujino,<sup>(3)</sup> K. K. Gan,<sup>(3)</sup> E. Gero,<sup>(7)</sup> G. Gidal,<sup>(1)</sup> T. Glanzman,<sup>(3)</sup> G. Goldhaber,<sup>(1)</sup> J. J. Gomez Cadenas,<sup>(2)</sup> G. Gratta,<sup>(2)</sup> G. Grindhammer,<sup>(3)</sup> P. Grosse-Wiesmann,<sup>(3)</sup> G. Hanson,<sup>(3)</sup> R. Harr,<sup>(1)</sup> B. Harral,<sup>(6)</sup> F. A. Harris,<sup>(8)</sup> C. M. Hawkes,<sup>(5)</sup> K. Hayes,<sup>(3)</sup> C. Hearty,<sup>(1)</sup> C. A. Heusch,<sup>(2)</sup> M. D. Hildreth,<sup>(3)</sup> T. Himel,<sup>(3)</sup> D. A. Hinshaw,<sup>(9)</sup> S. J. Hong,<sup>(7)</sup> D. Hutchinson,<sup>(3)</sup> J. Hysten,<sup>(6)</sup> W. R. Innes,<sup>(3)</sup> R. G. Jacobsen,<sup>(3)</sup> J. A. Jaros,<sup>(3)</sup> C. K. Jung,<sup>(3)</sup> J. A. Kadyk,<sup>(1)</sup> J. Kent,<sup>(2)</sup> M. King,<sup>(2)</sup> S. R. Klein,<sup>(3)</sup> D. S. Koetke,<sup>(3)</sup> S. Komamiya,<sup>(3)</sup> W. Koska,<sup>(7)</sup> L. A. Kowalski,<sup>(3)</sup> W. Kozanecki,<sup>(3)</sup> J. F. Kral,<sup>(1)</sup> M. Kuhlen,<sup>(5)</sup> L. Labarga,<sup>(2)</sup> A. J. Lankford,<sup>(3)</sup> R. R. Larsen,<sup>(3)</sup> F. Le Diberder,<sup>(3)</sup> M. E. Levi,<sup>(1)</sup> A. M. Litke,<sup>(2)</sup> X. C. Lou,<sup>(4)</sup> V. Lüth,<sup>(3)</sup> J. A. McKenna,<sup>(5)</sup> J. A. J. Matthews,<sup>(6)</sup> T. Mattison,<sup>(3)</sup> B. D. Milliken,<sup>(5)</sup> K. C. Moffeit,<sup>(3)</sup> C. T. Munger,<sup>(3)</sup> W. N. Murray,<sup>(4)</sup> J. Nash,<sup>(3)</sup> H. Ogren,<sup>(4)</sup> K. F. O'Shaughnessy,<sup>(3)</sup> S. I. Parker,<sup>(8)</sup> C. Peck,<sup>(5)</sup> M. L. Perl,<sup>(3)</sup> F. Perrier,<sup>(3)</sup> M. Petradza,<sup>(3)</sup> R. Pitthan,<sup>(3)</sup> F. C. Porter,<sup>(5)</sup> P. Rankin,<sup>(9)</sup> K. Riles,<sup>(3)</sup> F. R. Rouse,<sup>(3)</sup> D. R. Rust,<sup>(4)</sup> H. F. W. Sadrozinski,<sup>(2)</sup> M. W. Schaad,<sup>(1)</sup> B. A. Schumm,<sup>(1)</sup> A. Seiden,<sup>(2)</sup> J. G. Smith,<sup>(9)</sup> A. Snyder,<sup>(4)</sup> E. Soderstrom,<sup>(5)</sup> D. P. Stoker,<sup>(6)</sup> R. Stroynowski,<sup>(5)</sup> M. Swartz,<sup>(3)</sup> R. Thun,<sup>(7)</sup> G. H. Trilling,<sup>(1)</sup> R. Van Kooten,<sup>(3)</sup> P. Voruganti,<sup>(3)</sup> S. R. Wagner,<sup>(3)</sup> S. Watson,<sup>(2)</sup> P. Weber,<sup>(9)</sup> A. Weigend,<sup>(3)</sup> A. J. Weinstein,<sup>(2)</sup> A. J. Weir,<sup>(5)</sup> E. Wicklund,<sup>(5)</sup> M. Woods,<sup>(3)</sup> D. Y. Wu,<sup>(5)</sup> M. Yurko,<sup>(4)</sup> C. Zaccardelli,<sup>(2)</sup> and C. von Zanthier<sup>(2)</sup>

<sup>(1)</sup>Lawrence Berkeley Laboratory and Department of Physics,  
University of California, Berkeley, California 94720

<sup>(2)</sup>University of California at Santa Cruz, Santa Cruz, California 95064

<sup>(3)</sup>Stanford Linear Accelerator Center, Stanford University, Stanford, California 94309

<sup>(4)</sup>Indiana University, Bloomington, Indiana 47405

<sup>(5)</sup>California Institute of Technology, Pasadena, California 91125

<sup>(6)</sup>Johns Hopkins University, Baltimore, Maryland 21218

<sup>(7)</sup>University of Michigan, Ann Arbor, Michigan 48109

<sup>(8)</sup>University of Hawaii, Honolulu, Hawaii 96822

<sup>(9)</sup>University of Colorado, Boulder, Colorado 80309

(Received 12 October 1989)

We have measured the mass of the Z boson to be  $91.14 \pm 0.12 \text{ GeV}/c^2$ , and its width to be  $2.42^{+0.13}_{-0.11} \text{ GeV}$ . If we constrain the visible width to its standard-model value, we find the partial width to invisible decay modes to be  $0.46 \pm 0.10 \text{ GeV}$ , corresponding to  $2.8 \pm 0.6$  neutrino species, with a 95%-confidence-level upper limit of 3.9.

PACS numbers: 14.80.Er, 13.38.+c, 13.65.+i

We present an improved measurement of the Z-boson resonance parameters. The measurement is based on a total of  $19 \text{ nb}^{-1}$  of data recorded at ten different center-of-mass energies between 89.2 and 93.0 GeV by the Mark II detector at the SLAC Linear Collider. This data sample represents approximately 3 times the integrated luminosity presented in an earlier Letter.<sup>1</sup> The statistical significance of the luminosity measurement is further improved by including a detector component—the mini-small-angle monitor (MiniSAM)—not used in the previous analysis. The larger data sample and improved luminosity measurement result in a significant reduction in the resonance-parameter uncertainties. In particular, our observations exclude the presence of a fourth standard-model massless neutrino species at a confidence level of 95%.

The Mark II drift chamber and calorimeters provide the principal information used to identify Z decays.<sup>2</sup> Charged particles are detected and momentum analyzed in a 72-layer cylindrical drift chamber in a 4.75-kG axial magnetic field. The drift chamber tracks charged particles with  $|\cos\theta| < 0.92$ , where  $\theta$  is the angle to the incident beams. Photons are detected in electromagnetic calorimeters that cover the region  $|\cos\theta| < 0.96$ . The calorimeters in the central region (barrel calorimeters) are lead-liquid-argon ionization chambers, while the end-cap calorimeters are lead-proportional-tube counters.

There are two detectors for the small-angle  $e^+e^-$  (Bhabha) events used to measure the integrated luminosity. The small-angle monitors (SAM's) cover the angular region of  $50 < \theta < 160 \text{ mrad}$ . Each SAM consists of

nine layers of drift tubes for tracking (not used in this analysis) and a six-layer lead-proportional-tube sandwich for measuring the electron energy and position. The MiniSAM's detect Bhabha events in the region  $15.2 < \theta < 25.0$  mrad at one end of the detector and  $16.2 < \theta < 24.5$  mrad at the other. Each MiniSAM is a 15-radiation-length-thick tungsten-scintillator sandwich divided into four azimuthal quadrants.

The center-of-mass energy ( $E$ ) is determined on every pulse with an uncertainty of 35 MeV using an energy spectrometer in the extraction line of each beam.<sup>3</sup> The center-of-mass energy spread, which is typically 250 MeV, is determined to approximately 30% of its value.<sup>4</sup>

The Mark II data-acquisition system contains two redundant triggers for  $Z$  decays. The charged-particle trigger requires two or more charged tracks with transverse momenta greater than about 150 MeV/ $c$  and  $|\cos\theta| < 0.75$ . The neutral-energy trigger fires on a single shower depositing at least 3.3 GeV in the barrel calorimeter of 2.2 GeV in an end-cap calorimeter. Monte Carlo (MC) simulations indicate that 99.8% of hadronic  $Z$  decays will satisfy at least one of the triggers.<sup>5</sup> Of the 450 hadronic events in our data sample, 446 satisfied both triggers. Depositions of at least 6 GeV in each SAM or 20 GeV in each MiniSAM also satisfy the data-acquisition trigger.

We require candidates for  $Z$  hadronic decays to have at least three charged tracks and at least  $0.05E$  of energy visible in each of the forward and backward hemispheres. The reconstructed charged tracks are required to emerge with transverse momenta greater than 110 MeV/ $c$  at  $|\cos\theta| < 0.92$  from a cylindrical volume of radius 1 cm and half-length 3 cm parallel to the beam line. A MC simulation indicates that we expect 0.02 event in our data from two-photon-exchange interactions. The number of beam-gas interactions that satisfy these cuts is expected to be  $< 0.2$  at the 90% confidence level (C.L.) since no events are found emerging from the beam line with  $3 < |z| < 50$  cm. The efficiency for  $Z$  hadronic decays to satisfy these selection requirements, including trigger, is found by MC simulation to be  $\epsilon_h = 0.953 \pm 0.006$ . Differences between QCD models account for the largest component of the uncertainty. Backgrounds from the beam are included in the MC detector simulation by combining data from random beam crossings with MC events. They are found to have little effect on the analysis.

We also include in our fiducial sample  $\mu$  and  $\tau$  pairs with  $|\cos\theta_T| < 0.65$ , where  $\theta_T$  is the thrust angle. In this angular region, the trigger efficiency for leptonic events is high and the identification is unambiguous.  $\tau$  events are required to have visible energy greater than  $0.1E$ . The efficiencies for events in the fiducial angular region are found by MC simulation to be  $\epsilon_\mu = (99 \pm 1)\%$  and  $\epsilon_\tau = (96 \pm 1)\%$ .  $\tau$  events at  $|\cos\theta_T| > 0.65$  that satisfy the hadronic selection criteria are rejected by a handscan.

Bhabha-scattering events in the SAM calorimeters ( $50 < \theta < 160$  mrad) are selected by requiring 40% of the beam energy in each SAM. There is negligible background to these events. The cross section for these "inclusive" events is derived by scaling—using data from all center-of-mass energies—to the subset of events that fall into a smaller fiducial volume that has an accurately calculable acceptance. These "precise" Bhabha events are those for which  $65 < \theta < 160$  mrad for both  $e^-$  and  $e^+$  showers, plus, with a weight of 0.5, events where one shower is within the precise region and the other shower has  $60 < \theta < 65$  mrad. This weighting reduces the effects of misalignments and detector resolution. The theoretically expected cross section<sup>6</sup> for events to be observed in the precise angular region is  $25.2 \times [91.1/E \text{ (GeV)}]^2$  nb. This includes a  $-1.9\%$  correction for reconstruction inefficiency and a  $+1.6\%$  correction for detector-resolution effects. The estimated systematic errors are 2% from unknown higher-order radiative corrections and 2% due to detector resolution and reconstruction effects. Scaling by the ratio of inclusive to precise events gives a cross section for the production of events selected as inclusive Bhabhas events of  $\sigma_S = 42.6 \times [91.1/E \text{ (GeV)}]^2$  nb, with a 2.9% statistical error due to the scaling factor. A realignment of the synchrotron radiation masking, performed after the first seven energy-scan points, decreased  $\sigma_S$  by  $(1 \pm 2)\%$  for subsequent data. This factor is included in all of the following calculations.

To select Bhabha events in the MiniSAM, we require that a pair of adjacent quadrants on each sides of the interaction point (IP) contain at least 25 GeV more deposited energy than the other pair of quadrants on that side. The pairs with significant energy must be diagonally opposite. In addition, all quadrants with greater than 18-GeV deposited energy must have timing information consistent with particles coming from the IP rather than striking the back of the detector 14 ns earlier. The efficiency ( $\epsilon_M$ ) for each energy-scan point is derived by combining random beam crossings at that energy with Monte Carlo Bhabha events. It varies from 91% to  $> 99\%$ . Events in which the high-energy pairs are not diagonally opposite are used to estimate the number of beam related background events to be subtracted. The subtraction, which is 0.4% overall, ranges from 0% to 3.5% of the data at each scan point and is always less than the statistical error. The uncertainty in the number subtracted is taken to be the larger of 1% of the data or the number itself. Because of sensitivity to higher-order radiative corrections and slight misalignments of the defining masks, we do not directly calculate the production cross section for MiniSAM Bhabha events, but instead find it by scaling the efficiency corrected number of events to the SAM inclusive events. For the first seven scan points,  $\sigma_M = 227 \times [91.1/E \text{ (GeV)}]^2$  nb, while for the subsequent data,  $\sigma_M = 234 \times [91.1/E \text{ (GeV)}]^2$  nb. In both cases, there is an independent 4.5% statistical error

due to the scaling factor.

Table I gives, for each scan point, the mean energy of the Bhabha events as measured by the energy spectrometer, the number of SAM inclusive ( $N_S$ ) and MiniSAM ( $N_M$ ) Bhabha events,  $\epsilon_M$ , the integrated luminosity, the number of hadronic and leptonic  $Z$  decays detected that satisfy the fiducial requirements, and  $\sigma_Z$ . The cross sections  $\sigma_Z$  are for the production of hadronic events and muon and  $\tau$  pairs with  $|\cos\theta_T| < 0.65$ . The average  $\sigma_E$  generated by the energy spread of the beams and by the pulse-to-pulse jitter and drifts of the beam energies varies from 0.22 to 0.29 GeV. The cross sections contain corrections for this energy spread that vary from +3% near the peak to -3% in the tails.

The visible  $Z$  cross section ( $\sigma_Z$ ) can be represented by a relativistic Breit-Wigner resonance shape:

$$\sigma_Z(E) = \frac{12\pi}{m_Z^2} \frac{s\Gamma_e\Gamma_f}{(s - m_Z^2)^2 + s^2\Gamma^2/m_Z^2} [1 + \delta(E)], \quad (1)$$

where  $s \equiv E^2$ ,  $\delta$  is the substantial correction due to initial-state radiation calculated using an analytic form,<sup>7</sup>  $\Gamma_e$  is the  $Z$  partial width for electron pairs, and  $\Gamma_f$  is the partial width for decays in our fiducial volume. The partial widths for hadrons, muons, and  $\tau$ 's are related to  $\Gamma_f$  by  $\Gamma_f = \Gamma_h + f(\Gamma_\mu + \Gamma_\tau)$ , where  $f = 0.556$  is the fraction of all muon and  $\tau$  decays that have  $|\cos\theta_T| < 0.65$ . We take the total  $Z$  width to be  $\Gamma = \Gamma_h + \Gamma_e + \Gamma_\mu + \Gamma_\tau + N_\nu\Gamma_\nu$ , where  $N_\nu$  is the number of species of neutrinos.

We estimate  $Z$  resonance parameters by constructing a likelihood function from the probability of observing, at each energy,  $n_Z$   $Z$  decays and  $n_L$  SAM and MiniSAM Bhabha events given that we have observed a total of  $n_Z + n_L$  events. After eliminating terms that are constant with respect to the fit parameters we obtain for the

likelihood  $L$

$$L = \prod \frac{(\epsilon\sigma_Z)^{n_Z}}{(\epsilon\sigma_Z + \sigma_L)^{n_Z + n_L}}. \quad (2)$$

The product is over energy bins. The overall efficiency is  $\epsilon = 0.954$ . We take the C.L. corresponding to  $n$  standard deviations to be the point at which  $\ln L$  decreases by  $n^2/2$  from its maximum value.

We have performed three fits to the data, which differ in their reliance on the minimal standard model. The first leaves only  $m_Z$  as a free parameter. The widths are those expected for  $Z$  couplings to the known fermions (five quarks and three lepton doublets), including a QCD correction to the hadronic width.<sup>8</sup> The second fit leaves both  $m_Z$  and  $N_\nu$  as free parameters but fixes  $\Gamma_\nu$  and all other partial widths to their expected values. With this parametrization,  $N_\nu$  is derived largely from the height of the resonance. Finally, the third fit does not assume any standard-model partial widths. Instead, we write

$$\sigma_Z(E) = \sigma_0 \frac{s\Gamma^2}{(s - m_Z^2)^2 + s^2\Gamma^2/m_Z^2} [1 + \delta(E)], \quad (3)$$

and fit for  $m_Z$ ,  $\Gamma$ , and  $\sigma_0$  (peak production cross section, in the absence of radiative corrections, for all hadronic events and for muon and  $\tau$  pairs with  $|\cos\theta_T| < 0.65$ ) as the three fit parameters. The extracted values of  $N_\nu$  or  $\sigma_0$  depend on the value of  $\epsilon$  and the absolute luminosity normalization scale, while  $m_Z$  and  $\Gamma$  are not sensitive to these quantities.

The results of these fits are displayed in Fig. 1 and Table II. We conclude that  $m_Z = 91.14 \pm 0.12$  GeV/ $c^2$ . The uncertainty includes the contribution of 35 MeV due to the absolute energy measurement. The systematic error in  $m_Z$  due to uncertainty in the initial-state radiation

TABLE I. Average energy, integrated luminosity, number of events, MiniSAM efficiency, and  $\sigma_Z$  for each energy-scan point. The luminosity for each scan point is given by  $\mathcal{L} = (N_S + N_M)/\sigma_L$ , where  $\sigma_L = \sigma_S + \epsilon_M\sigma_M$ . The given error is the statistical error on  $N_S$  and  $N_M$  only; there are additional statistical errors on  $\sigma_L$  due to the scaling errors on  $\sigma_S$  and  $\sigma_M$  (see text). The total luminosity is calculated from the 485 "precise" SAM Bhabha events and has an overall 2.8% systematic error.

Scan point	$\langle E \rangle$ (GeV)	$N_S$	$N_M$	$\epsilon_M$	$\mathcal{L}$ (nb <sup>-1</sup> )	Z decays			$\sigma_Z$ (nb)
						Had.	Lep.	Tot.	
3	89.24	24	166	0.99	$0.68 \pm 0.05$	3	0	3	$4.5 \pm 1.3$
5	89.98	36	174	0.99	$0.76 \pm 0.05$	8	2	10	$18.5 \pm 4.9$
10	90.35	116	617	1.00	$2.61 \pm 0.10$	60	2	62	$24.8 \pm 3.8$
2	90.74	54	266	0.96	$1.21 \pm 0.07$	33	3	36	$31.7 \pm 9.8$
7	91.06	170	923	0.99	$4.08 \pm 0.12$	114	6	120	$31.6 \pm 3.4$
8	91.43	164	879	0.91	$4.12 \pm 0.13$	108	6	114	$29.8 \pm 3.3$
4	91.50	53	275	0.99	$1.23 \pm 0.07$	33	6	39	$34.3 \pm 7.9$
1	92.16	31	105	0.97	$0.54 \pm 0.05$	11	0	11	$21.5 \pm 6.6$
9	92.22	128	680	0.98	$3.05 \pm 0.11$	67	4	71	$24.3 \pm 3.6$
6	92.96	39	214	0.98	$1.00 \pm 0.07$	13	1	14	$14.6 \pm 4.6$
Totals		815	4299		$19.3 \pm 0.9$	450	30	480	

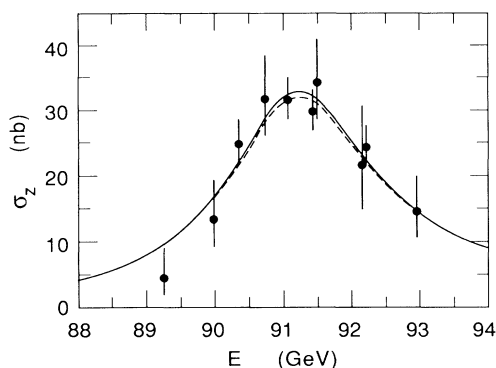


FIG. 1.  $e^+e^-$  annihilation cross sections to all hadronic events plus  $\mu$  and  $\tau$  pairs with  $|\cos\theta_T| < 0.65$ . The dashed curve represents the result of the first fit. The solid curve represents the second- and third-fit results, which are indistinguishable.

correction is estimated to be less than  $10 \text{ MeV}/c^2$ .<sup>7</sup> Previous direct measurements of  $m_Z$  by  $p\bar{p}$  colliders yielded  $93.1 \pm 1.0 \pm 3.1 \text{ GeV}/c^2$  (UA1),<sup>9</sup>  $91.5 \pm 1.2 \pm 1.7 \text{ GeV}/c^2$  (UA2),<sup>10</sup> and  $90.9 \pm 0.3 \pm 0.2 \text{ GeV}/c^2$  (CDF),<sup>11</sup> where the first error is statistical and systematic and the second reflects the uncertainty in the overall mass scale.

The second fit gives  $N_\nu = 2.8 \pm 0.6$ , corresponding to a partial width to invisible decay modes of  $N_\nu \Gamma_\nu = 0.46 \pm 0.10 \text{ GeV}$ . The luminosity uncertainty contributes 0.45 to the error in  $N_\nu$ . The 95%-C.L. limit,  $N_\nu < 3.9$ , excludes to this level the presence of a fourth massless neutrino species within the standard-model framework. Previous measurements of  $N_\nu$  by detection of single photons in  $e^+e^-$  annihilation have given<sup>12</sup>  $N_\nu > 5.2$ .

The third fit yields  $\Gamma = 2.42^{+0.43}_{-0.33} \text{ GeV}$ , which should be compared to the standard-model value of 2.45 GeV. The MiniSAM background subtraction error, which is the largest systematic error, contributes 50 MeV to the uncertainty. Previous direct measurements have yielded  $\Gamma = 3.8 \pm 0.8 \pm 1.0 \text{ GeV}$  (CDF)<sup>11</sup> and upper limits at the 90% C.L. of 5.2 GeV (UA1)<sup>9</sup> and 5.6 GeV (UA2).<sup>10</sup> The third-fit value for  $\sigma_0$  of  $45 \pm 4 \text{ nb}$  agrees well with the value of 43.6 nb calculated using  $m_Z = 91.14 \text{ GeV}/c^2$  and standard-model partial widths. The corresponding cross section for hadron decays is  $42 \pm 4 \text{ nb}$ . The maximum production cross section (including radiative corrections), which occurs approximately 90 MeV above the pole due to initial-state radiation, is  $33 \pm 3 \text{ nb}$  for all events in our fiducial region, or  $31 \pm 3 \text{ nb}$  for hadronic events only.

This work was supported in part by Department of Energy Contracts No. DE-AC03-81ER40050 (California Institute of Technology), No. DE-AM03-76SF00010 (University of California, Santa Cruz), No. DE-AC02-

TABLE II.  $Z$  resonance parameters. The three fits are described in the text.

Fit	$m_Z$ ( $\text{GeV}/c^2$ )	$N_\nu$	$\Gamma$ (GeV)	$\sigma_0$ (nb)
1	$91.14 \pm 0.12$	...	...	...
2	$91.14 \pm 0.12$	$2.8 \pm 0.6$	...	...
3	$91.14 \pm 0.12$	...	$2.42^{+0.43}_{-0.33}$	$45 \pm 4$

86ER40253 (University of Colorado), No. DE-AC03-83ER40103 (University of Hawaii), No. DE-AC02-84ER40125 (Indiana University), No. DE-AC03-76SF00098 (LBL), No. DE-AC02-76ER01112 (University of Michigan), and No. DE-AC03-76SF00515 (SLAC), and by the National Science Foundation (Johns Hopkins University).

<sup>1</sup>G. S. Abrams *et al.*, Phys. Rev. Lett. **63**, 724 (1989). The results presented in this reference are superseded by this analysis.

<sup>2</sup>G. S. Abrams *et al.*, Nucl. Instrum. Methods Phys. Res., Sect. A **281**, 55 (1989).

<sup>3</sup>J. Kent *et al.*, SLAC Report No. SLAC-PUB-4922, 1989 (to be published). Studies of the effects of momentum dispersion have reduced its contribution to the systematic error from 30 to 12 MeV and reduced the total systematic error from 40 to 35 MeV; M. Levi, J. Nash, and S. Watson, Nucl. Instrum. Methods Phys. Res., Sect. A **281**, 265 (1989); M. Levi *et al.*, SLAC Report No. SLAC-PUB-4921, 1989 (to be published).

<sup>4</sup>There were a few events for which one of the spectrometer energies was not available. In these cases, the missing-energy measurement was supplied by an auxiliary system which had been calibrated to the energy spectrometer.

<sup>5</sup>The first energy-scan point at 92.2 GeV has a somewhat more restrictive trigger which lowered the efficiency by 1.1%.

<sup>6</sup>F. A. Berends, R. Kleiss, and W. Hollik, Nucl. Phys. **B304**, 712 (1988); S. Jadach and B. F. L. Ward, Phys. Rev. D (to be published).

<sup>7</sup>R. N. Cahn, Phys. Rev. D **36**, 2666 (1987), Eqs. (4.4) and (3.1); see J. Alexander *et al.*, Phys. Rev. D **37**, 56 (1988), for a comparison of different radiative-correction calculations.

<sup>8</sup>Widths are calculated using the program EXPOSTAR, assuming  $m_{\text{top}} = 100 \text{ GeV}/c^2$ ; D. C. Kennedy *et al.*, Nucl. Phys. **B321**, 83 (1989).

<sup>9</sup>C. Albajar *et al.*, CERN Report No. CERN-EP/88-168, 1988 (to be published).

<sup>10</sup>R. Ansari *et al.*, Phys. Lett. B **186**, 440 (1987).

<sup>11</sup>F. Abe *et al.*, Phys. Rev. Lett. **63**, 720 (1989).

<sup>12</sup>The combined ASP, MAC, and CELLO result is calculated in C. Hearty *et al.*, Phys. Rev. D **39**, 3207 (1989).